ELSEVIER

Contents lists available at ScienceDirect

# Biochemical and Biophysical Research Communications

journal homepage: www.elsevier.com/locate/ybbrc



# The structure of SecB/OmpA as visualized by electron microscopy: The mature region of the precursor protein binds asymmetrically to SecB

Ying Tang <sup>a,1</sup>, Xijiang Pan <sup>a,1</sup>, Phang C. Tai <sup>b</sup>, Sen-Fang Sui <sup>a,\*</sup>

a State-Key Laboratory of Biomembrane and Membrane Biotechnology, Center for Structural Biology, School of Life Science, Tsinghua University, Beijing 100084, China

#### ARTICLE INFO

Article history: Received 4 February 2010 Available online 17 February 2010

Keywords: SecB Precursor protein Mature region

#### ABSTRACT

SecB, a molecular chaperone in *Escherichia coli*, binds a subset of precursor proteins that are exported across the plasma membrane via the Sec pathway. Previous studies showed that SecB bound directly to the mature region rather than to the signal sequence of the precursor protein. To determine the binding pattern of SecB and the mature region of the preprotein, here, we visualized the structure of the SecB/OmpA complex by electron microscopy. This complex is composed by two parts: the main density represents one SecB tetramer and the unfolded part of OmpA wrapping round it; the elongated smaller density represents the rest of OmpA. Each SecB protomer makes a different contribution to the binding of SecB with OmpA. The binding pattern between SecB tetramer and OmpA is asymmetric.

© 2010 Elsevier Inc. All rights reserved.

## Introduction

SecB, a molecular chaperone, is required for the export of a subset of precursor proteins across the plasma membrane via a general secretory pathway in Escherichia coli. When released from ribosomes, the newly synthesized precursor proteins bind to SecB in a translocation-competent state [1–4]. SecB prevents premature folding of the precursor proteins in the cytoplasm and targets them to the Sec translocase via its high-affinity binding to SecA [5–7]. The interaction between SecB and these precursor proteins is a crucial feature of the Sec pathway, as translocation can occur only if the precursor proteins are in an extended conformation [8-10]. The interaction between SecB and the preprotein has been extensively studied. Previous studies showed that although SecB does not bind to the signal sequence of the precursor protein directly, it can recognize non-native conformations within the mature region of the precursor protein and bind with high affinity (the dissociation constant  $[K_d]$  is around 5-50 nM) [11-15]. The SecBbinding site in the mature region of the precursor protein is a stretch of approximately 150-170 amino acids spanning SecB [12,16–18]. As no crystal structure of SecB containing a precursor protein ligand is available, the exact mode of the SecB-preprotein interaction remains poorly understood [19-21]. In particular, the structural basis for the function of the SecB C-terminus in preprotein translocation is unclear.

Electron microscopy (EM) and single-particle analysis allow the direct visualization of macromolecular protein complexes in solu-

tion. As expected, we found that in the absence of the signal sequence, OmpA formed a stable complex with SecB. SecB bound the unfolded part of OmpA only; the rest of OmpA did not bind directly to SecB. The binding pattern between each SecB protomer and the unfolded portion of OmpA was asymmetric.

### Materials and methods

Materials. His<sub>6</sub>-tagged SecB [22], proOmpA [23], and SecA [24] were purified as described previously. Protein samples were analyzed by 15% SDS-PAGE. Ni-NTA was obtained from QIAGEN. Ni-NTA-Nanogold was obtained from Nanoprobes.

Sucrose gradient centrifugation. Twelve-milliliter liner 10–30% sucrose gradients in buffer A (20 mM HEPES–KOH, pH 7.4, 30 mM KCl, and 1 mM DTT) were prepared in ultracentrifuge tubes. Sucrose was pumped into the bottom of the tubes at a rate of 1.0 mL/min using a peristaltic pump. The 0.2-mL load solution was layered on top of the gradient and subjected to ultracentrifugation in a HITACHI P40ST rotor at 4 °C for 20 h at 36,000 rpm. The gradients were fractionated by pumping out the contents from the bottom at a rate of 1.5 mL/min.

Size-exclusion chromatography. Size-exclusion chromatography was performed using an AKTA purifier (GE Healthcare). A total of  $100~\mu L$  of each protein sample was loaded onto a Superdex 200 analytical size-exclusion column equilibrated with buffer A. Separation was carried out at  $4~^\circ C$  at 0.5~m L/min.

On-grid Ni-NTA-Nanogold labeling. SecB/OmpA or SecB/pro-OmpA was deposited onto thin carbon film-coated grids. The grids were incubated at room temperature for 30 min with Ni-NTA-Nanogold (diluted 1/10 in 150 mM NaCl, 20 mM Tris-HCl, and 1%

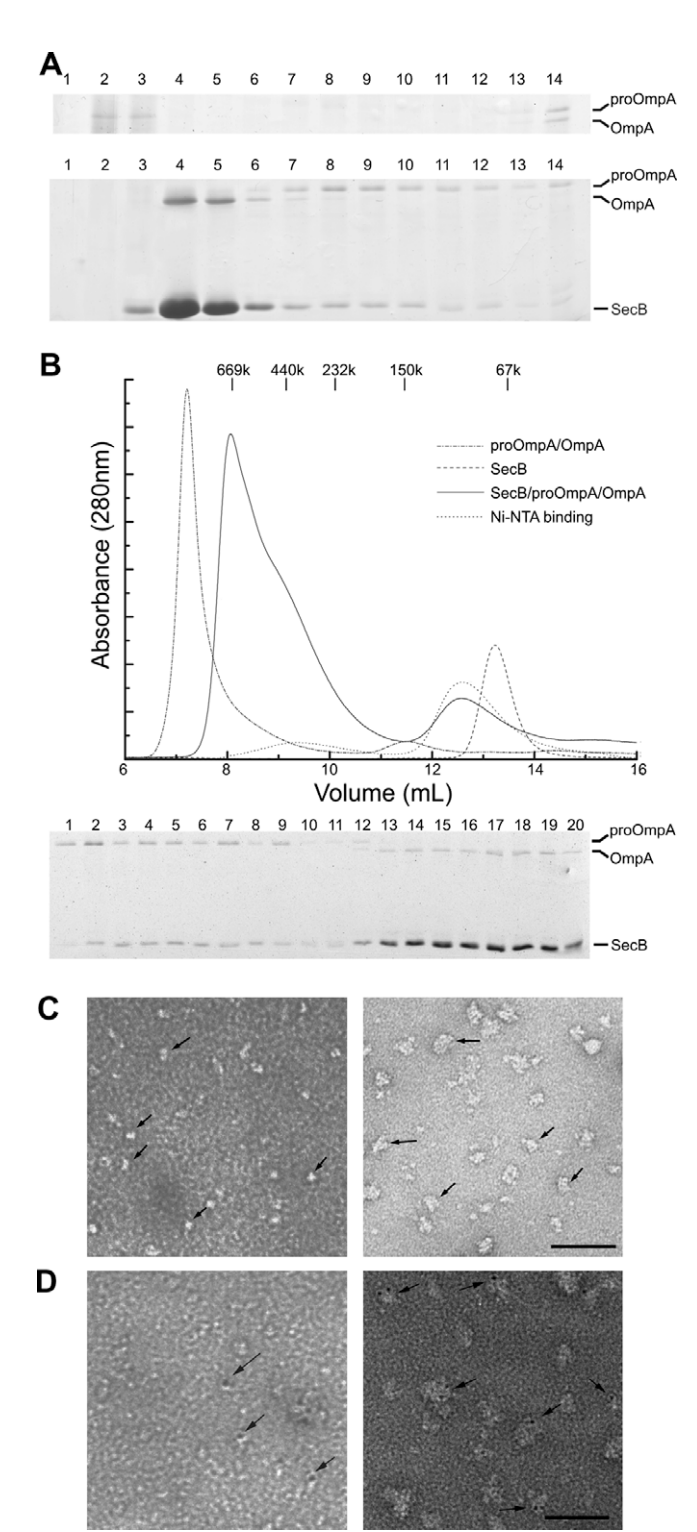
<sup>&</sup>lt;sup>b</sup> Department of Biology, Georgia State University, Atlanta, GA 30303, USA

<sup>\*</sup> Corresponding author. Fax: +86 10 62793367. E-mail address: suisf@mail.tsinghua.edu.cn (S.-F. Sui).

<sup>&</sup>lt;sup>1</sup> These authors are contributed equally to this work.

nonfat dried milk, pH 7.6). After incubation, the grids were washed with a buffer containing 300 mM NaCl, 50 mM Tris, and 20 mM imidazole adjusted to pH 7.6. Next, the grids were negatively stained.

Isothermal titration calorimetry (ITC). All calorimetric titrations were performed on a VP-ITC microcalorimeter (Microcal). Protein samples were extensively dialyzed against buffer B (50 mM HEPES and 50 mM KCl, pH 7.5). All solutions were filtered using membrane filters (pore size 0.22  $\mu m$ ) and thoroughly degassed



for 20 min by gentle stirring under a vacuum. For SecB–SecA, the 1.35-mL sample cell was filled with a 20-μM solution of SecA dimer and a 200-μM solution of SecB tetramer using a 250-μL injection syringe; for SecB/OmpA–SecA, the 1.35-mL sample cell was filled with a 10-μM solution of SecA and a 100-μM solution of SecB/OmpA complex using a 250-μL injection syringe. Each titration typically consisted of a preliminary 2-μL injection followed by 15 or 30 subsequent 12-μL injections. The data for the preliminary injections, which were affected by diffusion of the solution from and into the injection syringe during the initial equilibration period, were discarded. Binding isotherms were generated by plotting the heats of reaction normalized by the modes of injectant versus the ratio of total injectant to the total protein per injection. The data were fitted using Origin 7.0 (Microcal).

EM and three-dimensional (3D) reconstruction. For negative staining, a 5-uL sample was applied to a hydrophilic carbon-coated EM grid for 1 min and then stained with 1% uranyl acetate (w/v) for 1 min. The specimens were examined using a Phillips CM120 microscope operated at 100 kV. Images were recorded on Kodak SO-163 film at 74,000× magnification under low-dose conditions. Following development in full-strength D19 for 12 min, selected images were digitized with a Nikon Coolscan 9000ED scanner at a step size of 12.7 μm/pixel. Three-dimensional reconstructions were performed mainly using the EMAN package [25]. About 3510 particles were selected manually. The particle images were bandpass filtered, then centered and rotationally aligned using the CENALIGNINT command. About 10% of the particles were discarded after this step due to poor alignment. The remaining 3265 particles were classified into about 40 groups by multivariate statistical analysis. Eight typical class averages from the resulting 40 classes were selected, and an initial model was obtained by angular reconstitution. Back projections of this initial model were computed at 30° intervals, and a projection match was performed on the data set of 3265 particles over eight cycles. The final map was calculated from 2987 particles at 15° intervals. The resolution of the final map was estimated by both the Fourier Shell Correlation (FSC) and Differential Phase Residual (DPR) methods. The final 3D map was low-pass filtered at 2.4 nm and visualized by CHI-MERA [26]; the surface threshold was selected to fit the molecular weight of 103 kDa (sum of the SecB tetramer and OmpA) assuming a protein density of 1.35 g/mL.

Fig. 1. SecB can form a complex with proOmpA or OmpA. (A) A mixture of proOmpA and OmpA (50 µg) in 8-M urea was rapidly diluted into 0.2 mL of buffer A with or without SecB. The samples were then layered onto sucrose gradients and sedimented, as described in Materials and methods, Fractions (1 mL) were collected from the bottom of each gradient and analyzed by SDS-PAGE with Coomassie blue staining after TCA precipitation. The fraction numbers (1-14) are listed from the top to the bottom of the gradient. Top panel: no SecB present during rapid dilution. Bottom panel: SecB added (55 μg). (B) A mixture of OmpA and proOmpA (200 μg) was rapidly diluted into 200  $\mu\text{L}$  of buffer A with or without SecB and used for sizeexclusion chromatography. Dash line: SecB alone (12.5 µg). Dash dot line: no SecB present during rapid dilution. Solid line: SecB added (55 µg). Dot line: After rapid dilution with SecB. Ni-NAT was added to the preparation. The protein complexes were eluted with 250 mM imidazole in buffer A after binding at 4 °C for 60 min and were then applied to the column. Marker protein: albumin (67 kDa), aldolase (158 kDa), catalase (232 kDa), ferritin (440 kDa), and thyroglobulin (669 kDa). The elution fractions (300 µL/fraction, solid line) were collected and analyzed by SDS-PAGE after TCA precipitation with Coomassie blue staining. The panel shows the contents of 20 fractions (from 8.2 to 14.2 mL). (C) Negatively stained EM images of 20 μg/mL SecB/OmpA (left panel) and SecB/proOmpA (right panel) in buffer A. Several distinct complex particles are indicated by arrows. (D) Negatively stained EM images of Ni-NTA-Nanogold-labeled SecB/OmpA (left panel) and SecB/pro-OmpA (right panel). Several distinct Nanogold-labeled complex particles are indicated by arrows. The size bar corresponds to 50 nm in (C) and (D).

#### Results

SecB can form a complex with proOmpA or OmpA

ProOmpA was purified as a mixture with OmpA [23]. We monitored the formation of the SecB/proOmpA and SecB/OmpA complexes by sucrose gradient centrifugation (Fig. 1A). When the mixture of proOmpA and OmpA was diluted rapidly [2] from urea into buffer A without SecB, the two proteins were found in aggregates (Fig. 1A, upper panel). When SecB was included, both complexes could be formed and separated (Fig. 1A, lower panel). OmpA was found in a soluble form with SecB, indicating the formation of a complex between the two proteins. ProOmpA, unlike OmpA, was found in multiple lower fractions of the sucrose gradient with SecB. This suggested that the SecB/proOmpA complexes were heterogeneous and existed in more extended forms. We also examined the SecB/proOmpA and SecB/OmpA complexes by sizeexclusion chromatography (Fig. 1B). After rapid dilution, the preparation was applied to the column. The proOmpA/OmpA mixture without SecB was eluted at the void volume, indicating the formation of aggregates (Fig. 1B, dash dot line), consistent with our sucrose gradient data (Fig. 1A, upper panel). When the mixture was diluted with SecB, two peaks appeared, with the main peak shifted to a smaller size (Fig. 1B, solid line). The contents of each fraction (from 8.2 to 14.2 mL) were collected and analyzed by SDS-PAGE (Fig. 1B). The shoulder of the first peak contained SecB and pro-OmpA, whereas the second peak contained SecB and OmpA. The formation of SecB complexes was verified by Ni–NTA binding with His-tagged SecB after rapid dilution. Size-exclusion chromatography of the imidazole elution showed two peaks: SecB/proOmpA, corresponding to the shoulder (around 9.5 mL), and SecB/OmpA (at 12.5 mL) (Fig. 1B, dot line). The SecB/OmpA peak corresponded to an estimated molecular weight of 100 kDa, consistent with a single tetramer of SecB and one molecule of OmpA (calculated molecular weight: 103 kDa). These results suggest that SecB and OmpA form a stoichiometric complex.

Fractions containing the SecB/proOmpA and SecB/OmpA complexes collected by size-exclusion chromatography were immediately applied to EM grids and fixed by negative staining (Fig. 1C). SecB/proOmpA showed up as separate particles that varied in diameter from 10 to 50 nm. The observed variations in particle size and structural features suggest that SecB/proOmpA complexes are heterogeneous and complicated. On the other hand, SecB/OmpA showed well-preserved particles with a homogeneous structure. These results are supported by our Ni–NTA–Nanogold labeling analysis of His-tagged SecB (Fig. 1D). Both the homogeneous SecB/OmpA and heterogeneous SecB/proOmpA can be labeled by the Ni–NTA–Nanogold. These SecB/OmpA complexes were analyzed further.

The binding of SecB and SecB/OmpA to SecA was measured using ITC. ITC can measure changes in enthalpy occurring during

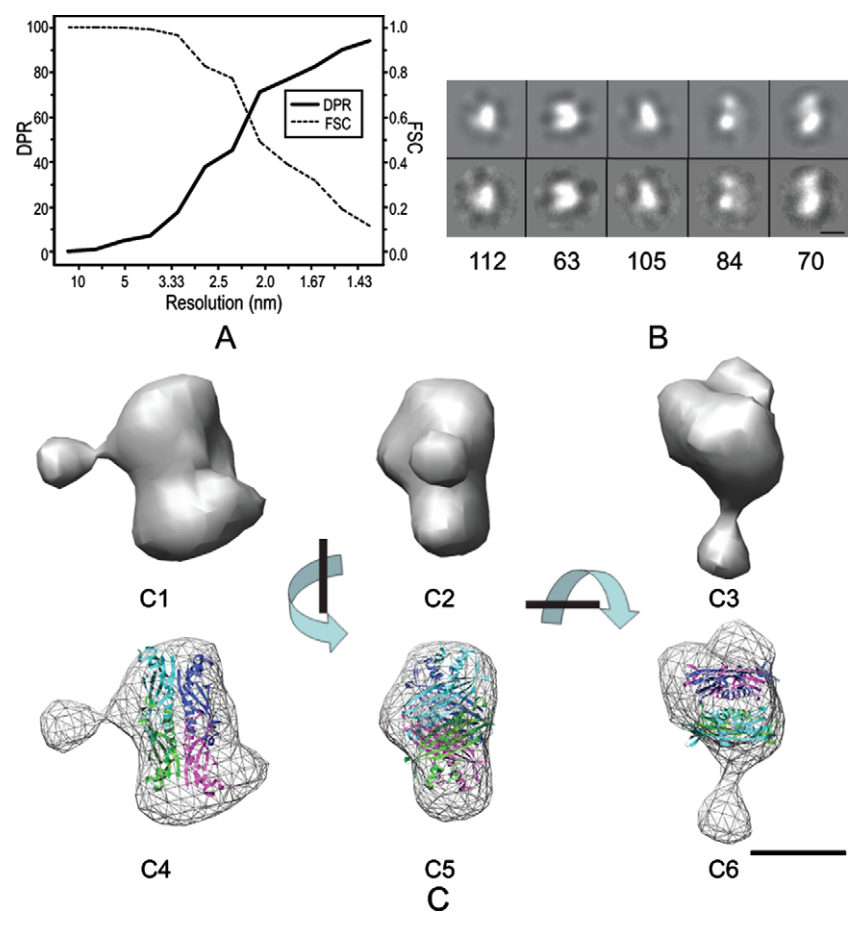


Fig. 2. Structure of the SecB/OmpA complex. (A) Resolution curves of the three-dimensional (3D) reconstruction as calculated by the Fourier Shell Correlation (FSC) (dashed line) and Differential Phase Residual (DPR) functions (solid line). (B) Distinct views of negatively stained SecB/OmpA EM samples. The top panel is the projection map of the reconstructed model; the bottom panel is the average map of all particles in this class. The number of particles in each class is indicated below the bottom panel. The size bar corresponds to 5 nm. (C) Surface representation of the 3D reconstruction of the SecB/OmpA complex (C1–C3) and docking of the Escherichia coli SecB X-ray structure into the EM 3D map (C4–C6). Top panel: surface representation of the 3D reconstruction. The surface was rendered and displayed using the chimera. Three views are shown: side (C1), top (C2), and bottom (C3). Each view was obtained after a 90° rotation around the axis, as shown between views. The bottom panel is shown for docking. The four SecB protomers are rendered in different colors: green, blue, cyan, and magenta. Each view is in the same orientation as its counterpart in the top panel. The size bar corresponds to 5 nm.

a bimolecular interaction as well as determine the  $K_{\rm d}$  and stoichiometries of the complexes. The mixture of proOmpA and OmpA, which was used as a control, showed no detectable binding with SecA by ITC (data not shown). Both SecB and SecB/OmpA showed significant changes in enthalpy, and therefore, clearly associate with SecA in solution. The  $K_{\rm d}$  between SecA and SecB was 2.045  $\mu$ M, whereas that between SecB/OmpA and SecA was 1.145  $\mu$ M (Supplementary Fig. S1). These data show that the mature region of proOmpA may contribute to the transfer of proOmpA from SecB to SecA.

Structure of the SecB/OmpA complex as analyzed by EM

Using single-particle EM we examined the structure of the SecB/OmpA particles. The particles displayed no preferred orientation on the grids (Supplementary Fig. S2). An angular reconstruction algorithm was used to produce the initial model, which was then refined by projection matching. A stable, asymmetric 3D model was obtained from 2987 negatively stained particles after twelve iterations of refinement. The resolution was estimated by comparing two independent data sets; a value of 2.1 nm was produced using the FSC criterion (>0.5), whereas a value of 2.4 nm was produced using the DPR criterion (<45°; Fig. 2A). The accuracy of the structure was assessed by comparing the class averages with the projections from the EM map at representative orientations (Fig. 2B and Supplementary Fig. S2). The reconstituted model, which lacked symmetry, has two parts: a main density and a smaller elongated density protruding from the main one (Fig. 2C).

We next manually docked the *E. coli* SecB crystal structures (PDB ID: 1QYN), which is organized as a dimer of dimers [19–21], into the EM density map to determine the localization of the molecules in the complex. The SecB tetramer could be fitted into the main density (Fig. 2C4–C6). The peripheral density wrapping around the SecB surface probably represents the unfolded portion of OmpA. The difference volume between the main density map and the low-pass filtered map of the SecB atomic model is much more around the green and magenta protomers than that around the blue and cyan ones (Supplementary Fig. S3). The elongated smaller density, which may represent the rest of OmpA, protrudes from the main density through one SecB dimer of the tetrmer (the cyan and green ones) (Fig. 2C4). This structure suggests that unfolded OmpA wraps asymmetrically around a single SecB tetramer.

## Discussion

In the Sec-dependent pathway, precursor proteins cannot be transported if they are folded or aggregated. The binding between the preprotein and SecB is a crucial step. For the first time, we visualized the structure of the SecB/OmpA complex by EM. Randall et al. showed that SecB bound directly to the mature regions of the preprotein rather than to the signal sequence and that the binding pattern between SecB and unfolded secretory proteins is the same with or without a signal peptide [11,27]. Thus, the SecB/OmpA complex structure may reveal the binding pattern between SecB and the preprotein. In the EM density, extended OmpA wraps around the SecB tetramer forming the main density, while the rest of OmpA protrudes. Our results are in agreement with those from a study of the binding pattern between SecB and another preprotein, MBP [28], and also the latest findings from Randall's group [27]. Lecker et al. reported that proOmpA contained secondary and tertiary structure prior to translocation when associated with SecB [3]. The protruding density may represent this structure. In the model, the peptidebinding groove and C-terminal tails of SecB, which were previously suggested to be the main preprotein binding sites, are covered by extended OmpA [19,20,27,29-31] (Supplementary Fig. S3). The most notable characteristic of the SecB/OmpA complex is that the density volume around each subunit is different and the smaller elongated domain protrudes through one SecB dimer. Each SecB protomer makes a different contribution to the binding of SecB to OmpA. These results suggest that the binding pattern between SecB tetramer and OmpA is asymmetric.

The two  $K_{\rm d}s$  produced by ITC indicate that SecA binds to SecB/OmpA with a greater affinity than to SecB alone. Thus, we suggest that, besides the signal sequence [5,32–34], the mature region of the preprotein may also contribute to the transfer of the preprotein from SecB to SecA.

Although proOmpA and OmpA can form complexes with SecB, a significant difference exists between the two complexes. Compared to the homogeneous SecB/OmpA complex, SecB/proOmpA was observed as heterogeneous particles by negatively-stained EM. The signal sequence may cause structural differences between the two complexes. Because the signal sequences of proOmpA do not bind to SecB directly, they may interact with each other or with the mature regions of proOmpA to avoid exposing their hydrophobic cores to an aqueous environment. Thus, the signal sequence may induce SecB and proOmpA to form heterogeneous oligomers rather than a stoichiometric complex like SecB/OmpA. The results of sucrose gradient centrifugation and size-exclusion chromatography (Fig. 1A and B) showed that the mole concentration of SecB to proOmpA was not 1:1. Our Ni-NTA binding and sucrose gradient centrifugation results suggest that free proOmpA may be mixed with SecB/proOmpA and that the interaction pattern between SecB and proOmpA may be more complicated than that of SecB/OmpA. Further structural study of SecB/proOmpA will elucidate the role of the signal sequence in the binding of SecB and the preprotein.

## Acknowledgments

We thank A.J. Driessen, H. Tokuda, and D. Oliver for providing the strains, Dr, Y.G. Shi and Dr. N. Yan for providing us the VP-ITC microcalorimeter and X.C. Li for technical assistance. This research was supported by National Natural Science Foundation of China (30830028) and National Basic Research program of China (2010CD833706/2010CB912400).

### Appendix A. Supplementary data

Supplementary data associated with this article can be found, in the online version, at doi:10.1016/j.bbrc.2010.02.062.

#### References

- [1] E. Breukink, R. Kusters, B. De Kruijff, In-vitro studies on the folding characteristics of the *Escherichia coli* precursor protein prePhoE. Evidence that SecB prevents the precursor from aggregating by forming a functional complex, Eur. J. Biochem. 208 (1992) 419–425.
- [2] S. Lecker, R. Lill, T. Ziegelhoffer, C. Georgopoulos, P.J. Bassford Jr., C.A. Kumamoto, W. Wickner, Three pure chaperone proteins of *Escherichia coli* SecB, trigger factor and GroEL form soluble complexes with precursor proteins in vitro, EMBO J. 8 (1989) 2703–2709.
- [3] S.H. Lecker, A.J. Driessen, W. Wickner, ProOmpA contains secondary and tertiary structure prior to translocation and is shielded from aggregation by association with SecB protein, EMBO J. 9 (1990) 2309–2314.
- [4] G. Liu, T.B. Topping, L.L. Randall, Physiological role during export for the retardation of folding by the leader peptide of maltose-binding protein, Proc. Natl. Acad. Sci. USA 86 (1989) 9213–9217.
- [5] P. Fekkes, J.G. de Wit, J.P. van der Wolk, H.H. Kimsey, C.A. Kumamoto, A.J. Driessen, Preprotein transfer to the *Escherichia coli* translocase requires the cooperative binding of SecB and the signal sequence to SecA, Mol. Microbiol. 29 (1998) 1179–1190.
- [6] F.U. Hartl, S. Lecker, E. Schiebel, J.P. Hendrick, W. Wickner, The binding cascade of SecB to SecA to SecY/E mediates preprotein targeting to the *E. Coli* plasma membrane, Cell 63 (1990) 269–279.
- [7] H.K. Hoffschulte, B. Drees, M. Muller, Identification of a soluble SecA/SecB complex by means of a subfractionated cell-free export system, J. Biol. Chem. 269 (1994) 12833–12839.

- [8] H. de Cock, W. Overeem, J. Tommassen, Biogenesis of outer membrane protein PhoE of *Escherichia coli*. Evidence for multiple SecB-binding sites in the mature portion of the PhoE protein, J. Mol. Biol. 224 (1992) 369–379.
- [9] L.L. Randall, S.J. Hardy, Correlation of competence for export with lack of tertiary structure of the mature species: a study in vivo of maltose-binding protein in *E. Coli*, Cell 46 (1986) 921–928.
- [10] J.B. Weiss, P.H. Ray, P.J. Bassford Jr., Purified secB protein of *Escherichia coli* retards folding and promotes membrane translocation of the maltose-binding protein in vitro, Proc. Natl. Acad. Sci. USA 85 (1988) 8978–8982.
- [11] L.L. Randall, T.B. Topping, S.J. Hardy, No specific recognition of leader peptide by SecB, a chaperone involved in protein export, Science 248 (1990) 860–863.
- [12] L.L. Randall, S.J. Hardy, High selectivity with low specificity: how SecB has solved the paradox of chaperone binding, Trends Biochem. Sci. 20 (1995) 65– 69.
- [13] L.L. Randall, T.B. Topping, S.J. Hardy, M.Y. Pavlov, D.V. Freistroffer, M. Ehrenberg, Binding of SecB to ribosome-bound polypeptides has the same characteristics as binding to full-length, denatured proteins, Proc. Natl. Acad. Sci. USA 94 (1997) 802–807.
- [14] T.B. Topping, L.L. Randall, Chaperone SecB from Escherichia coli mediates kinetic partitioning via a dynamic equilibrium with its ligands, J. Biol. Chem. 272 (1997) 19314–19318.
- [15] L.L. Randall, S.J. Hardy, T.B. Topping, V.F. Smith, J.E. Bruce, R.D. Smith, The interaction between the chaperone SecB and its ligands: evidence for multiple subsites for binding, Protein Sci. 7 (1998) 2384–2390.
- [16] T.B. Topping, L.L. Randall, Determination of the binding frame within a physiological ligand for the chaperone SecB, Protein Sci. 3 (1994) 730–736.
- [17] V.F. Smith, S.J. Hardy, L.L. Randall, Determination of the binding frame of the chaperone SecB within the physiological ligand oligopeptide-binding protein, Protein Sci. 6 (1997) 1746–1755.
- [18] V.J. Khisty, G.R. Munske, L.L. Randall, Mapping of the binding frame for the chaperone SecB within a natural ligand, galactose-binding protein, J. Biol. Chem. 270 (1995) 25920–25927.
- [19] C. Dekker, B. de Kruijff, P. Gros, Crystal structure of SecB from Escherichia coli, J. Struct. Biol. 144 (2003) 313–319.
- [20] Z. Xu, J.D. Knafels, K. Yoshino, Crystal structure of the bacterial protein export chaperone secB, Nat. Struct. Biol. 7 (2000) 1172–1177.
- [21] J. Zhou, Z. Xu, Structural determinants of SecB recognition by SecA in bacterial protein translocation, Nat. Struct. Biol. 10 (2003) 942–947.

- [22] J.P. Muller, J. Ozegowski, S. Vettermann, J. Swaving, K.H. Van Wely, A.J. Driessen, Interaction of *Bacillus subtilis* CsaA with SecA and precursor proteins, Biochem. J. 348 (Pt 2) (2000) 367–373.
- [23] K. Nishiyama, T. Suzuki, H. Tokuda, Inversion of the membrane topology of SecG coupled with SecA-dependent preprotein translocation, Cell 85 (1996) 71–81.
- [24] X. Chen, H. Xu, P.C. Tai, A significant fraction of functional SecA is permanently embedded in the membrane. SecA cycling on and off the membrane is not essential during protein translocation, J. Biol. Chem. 271 (1996) 29698–29706.
- [25] S.J. Ludtke, P.R. Baldwin, W. Chiu, EMAN: semiautomated software for highresolution single-particle reconstructions, J. Struct. Biol. 128 (1999) 82–97.
- [26] E.F. Pettersen, T.D. Goddard, C.C. Huang, G.S. Couch, D.M. Greenblatt, E.C. Meng, T.E. Ferrin, UCSF Chimera a visualization system for exploratory research and analysis, J. Comput. Chem. 25 (2004) 1605–1612.
- [27] A.A. Lilly, J.M. Crane, L.L. Randall, Export chaperone SecB uses one surface of interaction for diverse unfolded polypeptide ligands, Protein Sci. 18 (2009) 1860–1868.
- [28] P. Bechtluft, R.G. van Leeuwen, M. Tyreman, D. Tomkiewicz, N. Nouwen, H.L. Tepper, A.J. Driessen, S.J. Tans, Direct observation of chaperone-induced changes in a protein folding pathway, Science 318 (2007) 1458–1461.
- [29] J.M. Crane, Y. Suo, A.A. Lilly, C. Mao, W.L. Hubbell, L.L. Randall, Sites of interaction of a precursor polypeptide on the export chaperone SecB mapped by site-directed spin labeling, J. Mol. Biol. 363 (2006) 63–74.
- [30] D.L. Diamond, L.L. Randall, Kinetic partitioning. Poising SecB to favor association with a rapidly folding ligand, J. Biol. Chem. 272 (1997) 28994– 28998.
- [31] L.L. Randall, Peptide binding by chaperone SecB: implications for recognition of nonnative structure, Science 257 (1992) 241–245.
- [32] I. Gelis, A.M. Bonvin, D. Keramisanoù, M. Koukaki, G. Gouridis, S. Karamanou, A. Economou, C.G. Kalodimos, Structural basis for signal-sequence recognition by the translocase motor SecA as determined by NMR, Cell 131 (2007) 756– 769.
- [33] R. Lill, W. Dowhan, W. Wickner, The ATPase activity of SecA is regulated by acidic phospholipids, SecY, and the leader and mature domains of precursor proteins, Cell 60 (1990) 271–280.
- [34] C. Baud, S. Karamanou, G. Sianidis, E. Vrontou, A.S. Politou, A. Economou, Allosteric communication between signal peptides and the SecA protein DEAD motor ATPase domain, J. Biol. Chem. 277 (2002) 13724–13731.